Broadly tunable femtosecond Tm:Lu₂O₃ ceramic laser operating around 2070 nm

Alexander A. Lagatsky,[1,*] Oleg L. Antipov,[2] and Wilson Sibbett[1]

[1]*SUPA, School of Physics and Astronomy, University of St Andrews, North Haugh, St Andrews, KY16 9SS, UK*
[2]*Institute of Applied Physics of the Russian Academy of Sciences, 46 Ul'yanov Street,603950, Nizhny Novgorod, Russia*
[*]*aal2@st-andrews.ac.uk*

Abstract: Femtosecond mode locking of a Tm-doped Lu₂O₃ ceramic laser is reported. Transform-limited pulses as short as 180 fs are generated at 2076 nm with an average output power of 400 mW and a pulse repetition frequency of 121.2 MHz. An output power up to 750 mW can be reached at the somewhat longer pulse duration of 382 fs. Femtosecond pulse generation is realized in the 2030-2100 nm spectral range. Passive mode locking was achieved using an ion-implanted InGaAsSb quantum-well-based SESAM.

References and links

1. K. Petermann, L. Fornasiero, E. Mix, and V. Peters, "High melting sesquioxides: crystal growth, spectroscopy, and laser experiments," Opt. Mater. **19**(1), 67–71 (2002).
2. P. Klopp, V. Petrov, U. Griebner, K. Petermann, V. Peters, and G. Erbert, "Highly efficient mode-locked Yb:Sc₂O₃ laser," Opt. Lett. **29**(4), 391–393 (2004).
3. U. Griebner, V. Petrov, K. Petermann, and V. Peters, "Passively mode-locked Yb:Lu₂O₃ laser," Opt. Express **12**(14), 3125–3130 (2004).
4. C. R. E. Baer, C. Kränkel, C. J. Saraceno, O. H. Heckl, M. Golling, R. Peters, K. Petermann, T. Südmeyer, G. Huber, and U. Keller, "Femtosecond thin-disk laser with 141 W of average power," Opt. Lett. **35**(13), 2302–2304 (2010).
5. P. Koopmann, S. Lamrini, K. Scholle, P. Fuhrberg, K. Petermann, and G. Huber, "Efficient diode-pumped laser operation of Tm:Lu₂O₃ around 2 μm," Opt. Lett. **36**(6), 948–950 (2011).
6. P. Koopmann, S. Lamrini, K. Scholle, P. Fuhrberg, K. Petermann, and G. Huber, "Long wavelength laser operation of Tm:Sc₂O₃ at 2116 nm and beyond," in *Advanced Solid-State Photonics, Advances in Optical Materials, Fiber Laser Applications, High-Intensity Lasers and High-Field Phenomena* (ASSP/AIOM/FILAS/HILAS), (Optical Society of America, Washington, DC, 2011), ATuA5.
7. P. A. Budni, L. A. Pomeranz, M. L. Lemons, C. A. Miller, J. R. Mosto, and E. P. Chicklis, "Efficient mid-infrared laser using 1.9-μm-pumped Ho:YAG and ZnGeP₂ optical parametric oscillators," J. Opt. Soc. Am. B **17**(5), 723–728 (2000).
8. N. Leindecker, A. Marandi, R. L. Byer, K. L. Vodopyanov, J. Jiang, I. Hartl, M. Fermann, and P. G. Schunemann, "Octave-spanning ultrafast OPO with 2.6-6.1 μm instantaneous bandwidth pumped by femtosecond Tm-fiber laser," Opt. Express **20**(7), 7046–7053 (2012).
9. K. Scholle, E. Heumann, and G. Huber, "Single mode Tm and Tm,Ho:LuAG lasers for LIDAR applications," Laser Phys. Lett. **1**(6), 285–290 (2004).
10. R. C. Sharp, D. E. Spock, N. Pan, and J. Elliot, "190-fs passively mode-locked thulium fiber laser with a low threshold," Opt. Lett. **21**(12), 881–883 (1996).
11. K. Kieu and F. W. Wise, "Soliton thulium-doped fiber laser with carbon nanotube saturable absorber," IEEE Photon. Technol. Lett. **21**(3), 128–130 (2009).
12. M. Engelbrecht, F. Haxsen, A. Ruehl, D. Wandt, and D. Kracht, "Ultrafast thulium-doped fiber-oscillator with pulse energy of 4.3 nJ," Opt. Lett. **33**(7), 690–692 (2008).
13. F. Adler, P. Masłowski, A. Foltynowicz, K. C. Cossel, T. C. Briles, I. Hartl, and J. Ye, "Mid-infrared Fourier transform spectroscopy with a broadband frequency comb," Opt. Express **18**(21), 21861–21872 (2010).
14. M. J. Thorpe, D. Balslev-Clausen, M. S. Kirchner, and J. Ye, "Cavity-enhanced optical frequency comb spectroscopy: application to human breath analysis," Opt. Express **16**(4), 2387–2397 (2008).
15. B. Shan and Z. Chang, "Dramatic extension of the high-order harmonic cutoff by using a long-wavelength driving field," Phys. Rev. A **65**(1), 011804 (2001).
16. P. B. Corkum and F. Krausz, "Attosecond science," Nat. Phys. **3**(6), 381–387 (2007).

17. A. A. Lagatsky, P. Koopmann, P. Fuhrberg, G. Huber, C. T. A. Brown, and W. Sibbett, "Passively mode locked femtosecond $Tm:Sc_2O_3$ laser at 2.1 µm," Opt. Lett. **37**(3), 437–439 (2012).
18. A. Schmidt, P. Koopmann, G. Huber, P. Fuhrberg, S. Y. Choi, D.-II Yeom, F. Rotermund, V. Petrov, and U. Griebner, "175 fs $Tm:Lu_2O_3$ laser at 2.07 µm mode-locked using single-walled carbon nanotubes," Opt. Express **20**, 5313–5318 (2012).
19. J. Lu, J. F. Bisson, K. Takaichi, T. Uematsu, A. Shirakawa, M. Musha, K. Ueda, H. Yagi, T. Yanagitani, and A. A. Kaminskii, "$Yb^{3+}:Sc_2O_3$ ceramic laser," Appl. Phys. Lett. **83**(6), 1101–1103 (2003).
20. K. Takaichi, H. Yagi, A. Shirakawa, K. Ueda, S. Hosokawa, T. Yanagitani, and A. A. Kaminskii, "$Lu_2O_3:Yb^{3+}$ ceramics - a novel gain material for high-power solid-state lasers," Phys. Status Solidi **202**(1), R1–R3 (2005).
21. M. Tokurakawa, K. Takaichi, A. Shirakawa, K. Ueda, H. Yagi, S. Hosokawa, T. Yanagitani, and A. A. Kaminskii, "Diode-pumped mode-locked $Yb^{3+}:Lu_2O_3$ ceramic laser," Opt. Express **14**(26), 12832–12838 (2006).
22. M. Tokurakawa, K. Takaichi, A. Shirakawa, K. Ueda, H. Yagi, T. Yanagitani, and A. A. Kaminskii, "Diode-pumped 188 fs mode-locked $Yb^{3+}:Y_2O_3$ ceramic laser," Appl. Phys. Lett. **90**(7), 071101 (2007).
23. M. Tokurakawa, A. Shirakawa, K. Ueda, H. Yagi, T. Yanagitani, and A. A. Kaminskii, "Diode-pumped sub-100 fs Kerr-lens mode-locked $Yb^{3+}:Sc_2O_3$ ceramic laser," Opt. Lett. **32**(23), 3382–3384 (2007).
24. G. A. Newburgh, A. Word-Daniels, A. Michael, L. D. Merkle, A. Ikesue, and M. Dubinskii, "Resonantly diode-pumped $Ho^{3+}:Y_2O_3$ ceramic 2.1 µm laser," Opt. Express **19**(4), 3604–3611 (2011).
25. O. L. Antipov, S. Yu. Golovkin, O. N. Gorshkov, N. G. Zakharov, A. P. Zinov'ev, A. P. Kasatkin, M. V. Kruglova, M. O. Marychev, A. A. Novikov, N. V. Sakharov, and E. V. Chuprunov, "Structural, optical, and spectroscopic properties and efficient two-micron lasing of new $Tm^{3+}:Lu_2O_3$ ceramics," Quantum Electron. **41**(10), 863–868 (2011).
26. O. L. Antipov, A. A. Novikov, N. G. Zakharov, and A. P. Zinoviev, "Optical properties and efficient laser oscillation at 2066 nm of novel $Tm:Lu_2O_3$ ceramics," Opt. Mater. Express **2**(2), 183–189 (2012).
27. A. A. Lagatsky, F. Fusari, S. Calvez, S. V. Kurilchik, V. E. Kisel, N. V. Kuleshov, M. D. Dawson, C. T. A. Brown, and W. Sibbett, "Femtosecond pulse operation of a Tm,Ho-codoped crystalline laser near 2 microm," Opt. Lett. **35**(2), 172–174 (2010).
28. A. A. Lagatsky, X. Han, M. D. Serrano, C. Cascales, C. Zaldo, S. Calvez, M. D. Dawson, J. A. Gupta, C. T. A. Brown, and W. Sibbett, "Femtosecond (191 fs) $NaY(WO_4)_2$ Tm,Ho-codoped laser at 2060 nm," Opt. Lett. **35**(18), 3027–3029 (2010).
29. H. A. Haus, "Mode-locking of lasers," IEEE J. Quantum Electron. **6**(6), 1173–1185 (2000).
30. Y. Senatsky, A. Shirakawa, Y. Sato, J. Hagiwara, J. Lu, K. Ueda, H. Yagi, and T. Yanagitani, "Nonlinear refractive index of ceramic laser media and perspectives of their usage in a high-power laser-driver," Laser Phys. Lett. **1**(10), 500–506 (2004).
31. J. Ma, G. Q. Xie, P. Lv, W. L. Gao, P. Yuan, L. J. Qian, H. H. Yu, H. J. Zhang, J. Y. Wang, and D. Y. Tang, "Graphene mode-locked femtosecond laser at 2 µm wavelength," Opt. Lett. **37**(11), 2085–2087 (2012).

1. Introduction

Rare-earth ion doped crystalline sesquioxides RE_2O_3 (Re = Y, Sc, and Lu) offer attractive gain media options for high-power solid-state laser developments because of their superior thermo-mechanical properties. Indeed, the thermal conductivities of Sc_2O_3 and Lu_2O_3 crystals are 16.5 W/m·K and 12.5 W/m·K, respectively, and this is essentially unaffected with the rare-earth ion doping level in the case of Lu_2O_3. Additionally, due to strong electron-phonon interaction, a large splitting of the ground-state is observed and a moderate spectral broadening of the optical transitions takes place. These features are especially well suited to efficient laser operation under the quasi-three-level condition, broad tunability and further ultrashort-pulse generation [1–4]. Recently, efficient, high-power and broadly tunable (~1930-2150 nm) laser operation was demonstrated from Tm^{3+}-doped Lu_2O_3 and Sc_2O_3 continuous-wave (*cw*) lasers [5, 6]. Operation at these extended wavelengths from Tm-doped sesquioxides makes them attractive for a range of applications in molecular spectroscopy, as pump sources for optical parametric oscillators based on $ZnGeP_2$ [7] or GaAs [8] and for incorporation into LIDAR systems [9]. Moreover, it is also advantageous for stable passive mode locking because the presence of strong water vapor absorption bands in the ~1800-2000 nm region can prevent broadband mode locking and give rise to Q-switching instabilities.

The work on the development of ultrashort-pulse lasers that operate in the 2-µm spectral region is rather limited and based predominantly, to date, on fiber laser technology. Although Tm-doped or Tm-Ho co-doped fibre lasers operating around 2 µm exhibit excellent power scalability and efficiency in the *cw* regime, their performance characteristics during mode locking are rather restricted [10–12]. In this respect, Tm-doped sesquioxides represent excellent alternatives in the development of high-efficiency and high-power ultrashort-pulse oscillators operating in the 2-µm region. This is of particular interest for further developments

of mid-IR ultrafast broadband laser systems for molecular fingerprinting [13], trace gas detection [14], high-harmonic and X-ray generation [15] and attosecond science [16].

In our recently reported work [17], we have demonstrated passive mode locking of a $Tm:Sc_2O_3$ laser around 2.1 μm using InGaAsSb-based semiconductor saturable absorber mirror (SESAM) where pulses as short as 218 fs were produced with an average power of 210 mW. This was followed up by the passive mode locking of a $Tm:Lu_2O_3$ crystalline laser using a carbon nanotube saturable absorber from which 175-fs pulses were produced with an average power of 36 mW [18].

Interestingly, the attractive characteristics of rare-earth ion doped crystalline sesquioxides gain media have also led them to being studied extensively as ceramics. Currently, high optical quality sesquioxide ceramics can be produced by nanocrystalline and vacuum-sintering technologies. Such ceramic gain media possess stronger fracture toughness than single crystals and afford a high potential for size scalability thereby offering practical advantages in high-power laser implementations. Previously, a range of diode-pumped *cw* and ultrashort-pulse Yb-doped sesquioxides ceramic lasers have been demonstrated [19–23] and more recently high-power $Ho:Y_2O_3$ (*cw* operation) [24] and $Tm:Lu_2O_3$ (*cw* and Q-switched operation) [25,26] ceramic lasers operating around 2100 nm and 2070 nm, respectively, were reported.

Here we present, for the first time to our knowledge, research results on a passively mode-locked $Tm:Lu_2O_3$ ceramic laser. Transform-limited pulses of 180 fs duration were produced at 2070 nm with an average power up to 400 mW. The maximum output power of 750 mW was obtained during mode locking when the corresponding pulse duration was 382 fs. Tunability in the range of 2030-2100 nm was achieved for this $Tm:Lu_2O_3$ mode-locked laser .

2. Experimental results and discussion

2.1 Tm:Lu₂O₃ laser experimental setup and its cw performance

The experimental assessments were carried out with a Ti:sapphire pump laser that produced up to 2.6 W of output power at 796 nm. The gain medium was a 5-mm-long, Brewster-cut, 2 at % Tm-doped Lu_2O_3 ceramic rod. Its optical and spectroscopic properties have been previously reported [25, 26]. An asymmetric, astigmatically-compensated Z-fold resonator, described elsewhere [27, 28], was configured with two high-reflectivity (R > 99.8% from 1900 to 2100 nm) folding (full angle of 14°) mirrors having radii of curvature of 100 mm, an output coupler (OC) with 1.2%, 2.3%, or 4.3% transmission at around 2070 nm and a SESAM structure. The resonator was designed to operate in the middle of stability zone II to ensure a second mode waist on the saturable absorber. The SESAM used for initiating and stabilizing the passive mode locking is based on an ion-implanted InGaAsSb quantum-well structure having an initial reflectivity of 99.5-98.1% in the 2-2.1 μm range. To support a long-term stable laser operation both the gain element and the SESAM were mounted onto copper heat sinks that were maintained at 20°C using thermoelectric coolers. A *p*-polarized pump beam was focused into the gain medium via an 80-mm focal length lens and the folding mirror (*T* > 99% at 976 nm) to a spot radius of 26 μm ($1/e^2$ intensity) measured in air at the location of the input facet of the crystal. The laser beam mode radii inside the gain medium were calculated to be 32×61 μm^2.

During *cw* operation (a high-reflectivity plane mirror was used instead of SESAM and without the prism pair) the $Tm:Lu_2O_3$ ceramic laser produced a maximum output power of
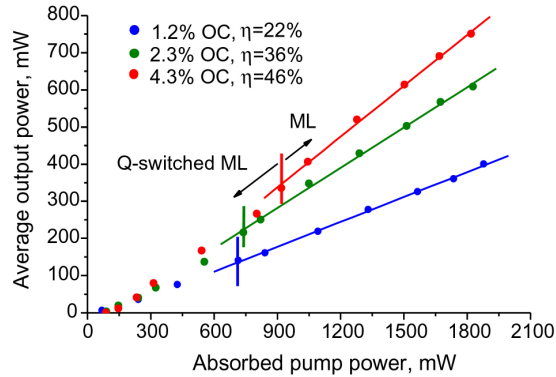
Fig. 1. Output power vs absorbed pump power characteristics of the Tm:Lu$_2$O$_3$ laser for different OCs during pulsed operation. The vertical lines indicate transitions from Q-switched mode locking to pure mode locking regimes.

930 mW at 2067 nm when the 4.3% OC was used and this corresponded to a slope efficiency of 54% (with respect to the absorbed pump power). With output couplings of 2.3% and 1.2% the average output powers reached 920 mW (52% slope efficiency) and 760 mW (43% slope efficiency), respectively, for the laser wavelengths around 2068 nm. The gain element absorbs about 70% of pump radiation during laser operation.

A pair of infrared-grade fused silica prisms with tip-to-tip separation of 12 cm was used to control the intracavity net group velocity dispersion (GVD). Each prism was placed at a minimum deviation to minimize the insertion losses. In particular, with the prism pair, the laser produced 900 mW, 820 mW and 640 mW with output couplings of 4.3%, 2.3% and 1.2%, respectively.

2.2 Mode locking results and analysis

Stable and self-starting passive mode locking of the Tm:Lu$_2$O$_3$ laser was realized when the intracavity beam mode size on the SESAM was set appropriately to overcome Q-switching instabilities on the one hand and to avoid multiple pulsing under maximum pump power conditions on the other. Figure 1 depicts the input-output characteristics of the Tm:Lu$_2$O$_3$ laser for three different output couplings with the SESAM in place. The maximum output power during mode locking of 750 mW was realized with the 4.3% OC and the laser operated with a slope efficiency of 46%. The cavity mode radii on the SESAM were set to be 135 μm, 158 μm and 175 μm for the 4.3%, 2.3% and 1.2% OCs respectively. Under these conditions, the thresholds for mode locking were similar for different output couplers, typically in the range of 100-107 μJ/cm^2 for the intracavity fluence on the SESAM, and single pulse stable operation was observed when the pump power was increased up to its maximum available level.

The temporal and spectral characteristics of the mode-locked Tm:Lu$_2$O$_3$ laser are as summarized in Fig. 2. The pulse duration was measured using intensity autocorrelator based on two-photon absorption effect in a Si-based detector, optical spectra were detected with a laser spectrometer having a resolution of 0.3 nm around 2-μm region (APE WaveScan) and the pulse repetition frequency was characterised by a fast (>7 GHz cut-off frequency) InGaAs photodetector in combination with a radio frequency spectrum analyzer (Rohde&Schwarz, FSP40). The shortest pulse duration of 180 fs was obtained with the 1.2% OC at a maximum average output power of 400 mW. The corresponding optical spectrum was centered at 2076 nm having a spectral width of 25.7 nm such that a time-bandwidth product of 0.32 was implied. When the output coupling was increased, longer pulse durations were observed. In
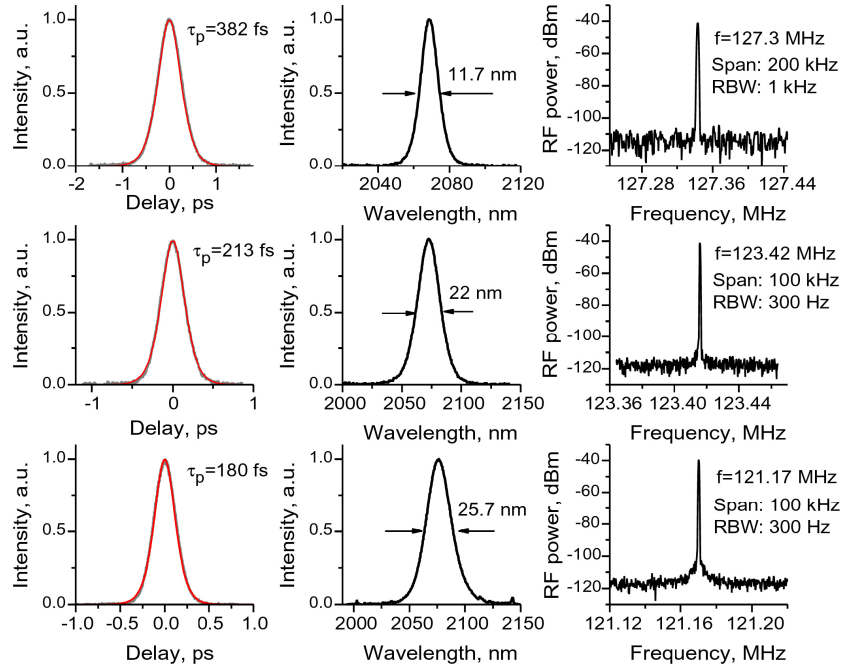
Fig. 2. Intensity autocorrelations, optical and radio frequency spectra (from left to right) of the mode-locked Tm:Lu$_2$O$_3$ laser with the 4.3% (top row), 2.3% (middle row) and 1.2% (bottom row) OCs.

particular, nearly transform-limited pulses of 213 fs and 382 fs duration were measured with the 2.3% and 4.3% OCs, respectively, for which optical spectra centered at 2072 nm and 2068 nm had the corresponding bandwidths of 22 nm and 11.7 nm. The average output powers reached of 608 mW (2.3% OC) and 750 mW (4.3% OC) that corresponds to generated pulse energies of 4.9 nJ and 5.9 nJ, respectively. The pulse repetition frequencies varied slightly in the range of 121.2-127.3 MHz as a result of different cavity lengths applying for specific output couplings that facilitated a required spot size on the SESAM.

A soliton mode locking regime was observed for all of the output coupling levels used and this is consistent with the dependence of the pulse duration on intracavity pulse energy (output power) and the net GVD. As a representative example, Fig. 3(a) depicts the variation of the pulse duration on the intracavity round-trip GVD which was increased from its initial value D_0 by insertion of a fused silica prism (−116 fs^2/mm at 2070 nm) at a fixed intracavity pulse energy of 214 nJ (2.3% OC, 608 mW average output power). From the linear fit to the experimental data the self-phase modulation coefficient δ could be deduced to be 4.6×10^{-7} W^{-1} using the well-known relationship between soliton pulse duration, pulse energy and GVD [29]. Complementarily, using the extracted value for δ and making the fit to the experimental data of the pulse duration versus the intracavity pulse energy at a fixed GVD (Fig. 3(b)) the value for D_0 was found to be −2980 fs^2. This is the total round-trip cavity GVD which, in this experimental setup, originates from the insertion of the prisms (glass material dispersion, -1392 fs^2), the gain medium itself (- 151 fs^2) and the angular dispersion of the prism pair (-1437 fs^2). Additionally, data deduced for the δ coefficient can provide an estimate for the nonlinear refractive index, n_2, of the gain medium according to the expression of $\delta = (2\pi/\lambda) \cdot (2L/A_{eff}) \cdot n_2$, where L is the length of the gain medium and A_{eff} if the effective mode area in the gain medium. The n_2 of the Tm:Lu$_2$O$_3$ ceramic at 2070 nm was thus calculated to be 3.3×10^{-16} cm^2/W. Previously, the nonlinear refractive index of the Lu$_2$O$_3$ ceramic was reported to be 8.6×10^{-16} cm^2/W at 1.06 μm [30].
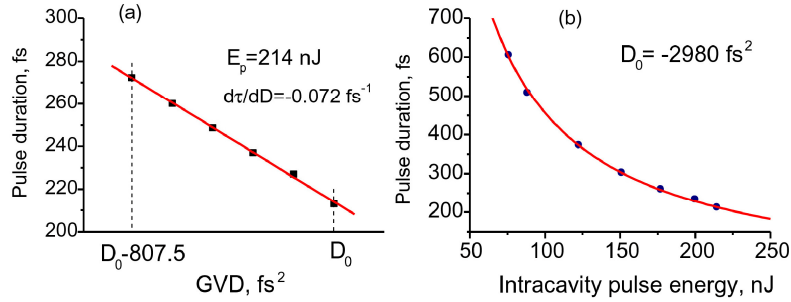
Fig. 3. Dependence of the pulse duration on (a) the intracavity GVD and (b) the intracavity pulse energy. The red curves are the best fits to the experimental data: $\tau \propto |D|$ in (a) and $\tau \propto 1/E_p$ in (b).

The tunability of the Tm:Lu$_2$O$_3$ ceramic laser during ultrashort pulse generation was measured with the 1.2% OC and using a single intracavity prism as a dispersive element. Stable and self-starting mode locking was realized in the 2030-2100 nm spectral range (Fig. 4) where the pulse durations varied from 370 fs at 2100 nm to 282 fs at 2030 nm with the maximum average output power of 450 mW achieved at around 2040 nm.
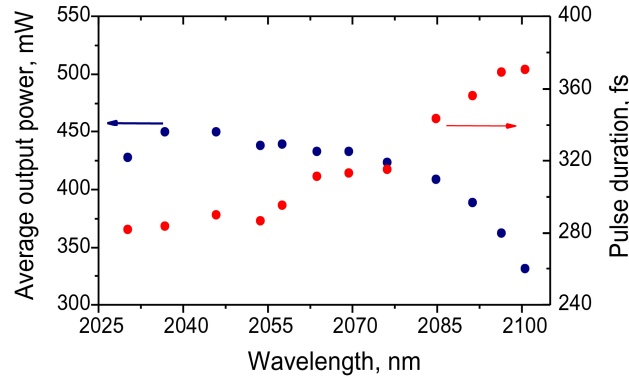

Fig. 4. Tunability of the mode-locked Tm:Lu$_2$O$_3$ ceramic laser.

3. Conclusion

In conclusion, efficient mode locking of a Tm:Lu$_2$O$_3$ ceramic laser in the femtosecond regime has been demonstrated for the first time to the authors' knowledge. Nearly transform-limited pulses as short as 180 fs were produced at 2076 nm with an average output power of 400 mW at a pulse repetition frequency of 121.2 MHz. When the average output power reached a maximum value of 750 mW during mode locking a pulse energy of 5.9 nJ was implied. We believe that further power and energy scaling from a femtosecond Tm:Lu$_2$O$_3$ ceramic laser is feasible with high-power laser diode pumping around 800 nm in combination with thin-disk cavity configurations. Also, it is expected that shorter pulse durations can be generated with optimized SESAM parameters or using more broadband and ultrafast absorbers based on graphene [31].

Acknowledgment